Determination of the crossover exponent in the random-field system $Mn_xZn_{1-x}F_2$

C. A. Ramos,* A. R. King, and V. Jaccarino
Department of Physics, University of California, Santa Barbara, California 93106
(Received 15 October 1987)

Optical birefringence (Δn) measurements have been used to study the antiferromagnetic phase boundary in the $d=3$ random-field Ising model (RFIM) system $Mn_xZn_{1-x}F_2$ ($x=0.40$, 0.55, and 0.83). From experiments at external fields $0\leq H\leq 20$ kOe, a value of the crossover exponent $\phi=1.43\pm0.03$ has been obtained. This agrees with both the value $\phi=1.42\pm0.03$ determined for the ideal RFIM system $Fe_xZn_{1-x}F_2$ and the one most recently obtained for $Fe_xMg_{1-x}Cl_2$, $\phi=1.41\pm0.05$. All satisfy the Aharony inequality $\phi>\gamma$, the $d=3$ random-exchange susceptibility exponent ($\gamma=1.31\pm0.03$). Thus all measured diluted antiferromagnets exhibit crossover from random-exchange (not *pure*) $d=3$ Ising model to RFIM behavior. We suggest possible misinterpretations in previous studies of the $Mn_xZn_{1-x}F_2$ and $Fe_xMg_{1-x}Cl_2$ systems that have led to the conclusion that the crossover was from pure to RFIM behavior. For the first time a quantitative analysis has been made of the field scaling of the peak amplitude and dynamical rounding of a thermodynamic function at the phase transition of the RFIM system.

I. INTRODUCTION

Random fields have profound effects on the ordering of magnetic systems. It is generally agreed that the lower critical dimension of the random-field Ising model (RFIM) is $d_l=2$. For $d>d_l$ new static and dynamic critical behavior is expected and is observed. However, no consensus exists as to all aspects of the phase transition, from either an experimental or theoretical point of view. Several factors contribute to the lack of unanimity in interpreting the experimental results on $d=3$ RFIM systems. The two most important factors are the extreme critical slowing down and macroscopic inhomogenity effects; the former prevents the system from equilibrating in the critical region, while the latter obscures the precise character of the critical behavior.

An additional element of ambiguity has been introduced by the fact that differing conclusions have been drawn from experimental studies of somewhat similar, but clearly not identical, $d=3$ RFIM systems. In every instance a diluted antiferromagnet in a uniform field has been studied, following the insight, first provided by Fishman and Aharony,[1] as to its equivalence to a random field applied to a pure ferromagnet. The most carefully characterized and extensively studied has been the $Fe_xZn_{1-x}F_2$ system.[2] Here the Ising character is derived from the very large, uniaxial, single-ion anisotropy. It most closely approximates the ideal $d=3$ RFIM system. Considerable attention has also been given to the isostructural $Mn_xZn_{1-x}F_2$,[3,4] although it possesses only a weak dipolar anisotropy. Lastly, some work has also been done on the $Fe_xMg_{1-x}Cl_2$ system[5,6] which is, in several ways, the least ideal of the three. Little attention has been given to the question of whether there are any intrinsic differences in the RFIM properties, either to be expected or to be observed, in the different systems. This is a major purpose of the present study.

Perhaps the first step in trying to establish whether such differences do exist would be to compare their crossover behavior, since one has only to determine the temperature at which the phase transition occurs as a function of field to obtain the crossover exponent ϕ. We have elected to do this rather than compare the more difficult to measure exponents associated with the static and dynamic critical behavior. If the crossover exponent is identical for all, then one expects the static and dynamical critical behavior should also be identical, since the crossover would be from and to the same universality class in each instance. Since this turns out to be case, it reinforces our previously held convictions that the $Fe_xZn_{1-x}F_2$ system is the best one in which to pursue definitive RFIM studies, as neither spin-flop nor metamagnetic transitions occur at relatively low values of the external field.

II. CROSSOVER TO RFIM BEHAVIOR

A. Static scaling

Fishman and Aharony[1] showed that an antiferromagnet with random exchange, when placed in a *uniform* field H, was physical realization of a random-field Ising model (RFIM) system. It was predicted that new critical behavior would be observed within a crossover region

$$|t|\leq t_{\rm cr}\propto h_{\rm RF}^{2/\phi}\ , \tag{1}$$

where $|t|\equiv|T-T_N+bH^2|/T_N$ is the reduced temperature measured relative to the mean-field phase boundary T_N-bH^2, $h_{\rm RF}$ is the reduced rms random field, and ϕ is the crossover exponent. The mean-square reduced random field for the site-diluted case has been shown to be, in the limit $h_{\rm RF}^2\ll 1$,[7]

$$h_{\mathrm{RF}}^2=\frac{x(1-x)[T_N^{\mathrm{MF}}(1)/T]^2(g\mu_B SH/k_BT)^2}{[1+\Theta^{\mathrm{MF}}(x)/T]^2}\ , \quad (2)$$

where $T_N^{\mathrm{MF}}(1)$ is the mean-field T_N in the pure system, and $\Theta^{\mathrm{MF}}(x)$ is the mean-field Curie-Weiss parameter. If a sharp phase transition exists, the new transition temperature is expected to occur at

$$T_c(H)=T_N-bH^2-cT_Nh_{\mathrm{RF}}^{2/\phi}\equiv T_N-bH^2-CH^{2/\phi}\ , \quad (3)$$

where c is a constant of order unity.

The magnetic specific heat C_m of a RFIM system is expected to scale as[1]

$$C_m(t,h_{\mathrm{RF}})=h_{\mathrm{RF}}^{-2\alpha/\phi}f(th_{\mathrm{RF}}^{-2/\phi})\ , \quad (4)$$

where α is the $H=0$ specific-heat exponent and f is a universal scaling function. Assuming a sharp phase transition exists at $T_c(H)$, this becomes, within the crossover region,

$$C_m\propto h_{\mathrm{RF}}^{2(\bar{\alpha}-\alpha)/\phi}\mid t-t_c\mid^{-\bar{\alpha}}\ , \quad (5)$$

where

$$t_c\equiv[T_c(H)-T_N+bH^2]/T_N=-ch_{\mathrm{RF}}^{2/\phi}\ ,$$

and $\bar{\alpha}$ is the RFIM specific-heat exponent. C_m exhibits a field-dependent scaling $C_m\propto h_{\mathrm{RF}}^{y}\mid t-t_c\mid^{-\bar{\alpha}}$, where[8] $y=2(\bar{\alpha}-\alpha)/\phi\simeq 0.13$. Although the temperature derivative of the optical birefrigence, $d(\Delta n)/dT$, has been shown to exhibit the same temperature divergence as does C_m, it is actually composed of two terms with different *field*-scaling exponents $y=0.13$ and $y'=(2/\phi)(1+\bar{\alpha}-\alpha)\simeq 1.56$, respectively.[8] Nevertheless, for values of the field energy which are small compared to the internal energy, $d(\Delta n)/dT$ appears to scale with external field as $\sim h_{\mathrm{RF}}^{0.13}$.

The actual value of the RFIM crossover exponent ϕ is of particular interest because here a distinction is to be made between the diluted antiferromagnet in a *uniform H* and the ferromagnet in a *random* field. For the ferromagnet the crossover proceeds from pure Ising to RFIM behavior and ϕ must be equal to γ_p, the *pure* Ising susceptibility exponent. Although the diluted antiferromagnet obviously corresponds to a system with random exchange, it was originally believed[1] that random-exchange Ising model (REIM) exponents would not be observable in the experimentally accessible critical region. It would follow that ϕ would again be equal to the *pure* Ising (not REIM) susceptibility exponent. The rationale behind this was the argument that the reduced crossover temperature t_{cr} from pure to REIM behavior should scale as

$$\mid t_{\mathrm{cr}}\mid\propto(\Delta J/J)^{1/\alpha}\propto(1-x)^{1/\alpha}\ , \quad (6)$$

where $\Delta J/J$ is the relative rms variation in the exchange, and α is the (pure) Ising specific-heat exponent $\alpha\sim 0.11$. Thus, for moderate dilution [where Eq. (6) was presumed to be valid], t_{cr} was expected to be so small as to be experimentally inaccessible. Consequently, the crossover to RFIM behavior would be described by $\phi=\gamma_p$.

However, more recent renormalization-group calculations have shown that the random-exchange fixed point occurs at fairly weak disorder;[9] the proportionality (6) should be replaced by

$$\mid t_{\mathrm{cr}}\mid\propto[(1-x)/(1-x_c)]^{1/\alpha}\ , \quad (7)$$

where experiment[10] suggests x_c might be as large as 0.9. In that case, the crossover from pure Ising to REIM behavior would be essentially complete for $x\lesssim 0.9$; thus REIM critical exponents should be and are[10,11,4] observable *and* the crossover is from REIM to RFIM behavior in this range.

Although the corssover is from REIM to RFIM behavior, it turns out that $\phi\neq\gamma$ (REIM). For the $d=3$ RFIM diluted antiferromagnet problem, Aharony has recently shown[12] that $\phi>\gamma$ and is bounded by

$$1.05\lesssim\phi/\gamma\lesssim 1.1\ . \quad (8)$$

Thus we have the following inequalities predicted for the $d=3$ REIM diluted antiferromagnet: $\phi>\gamma$ (REIM) $>\gamma_p$; with γ (REIM) $=1.31$ and $\gamma_p=1.24$. The experimental situation with respect to ϕ will be discussed after the presentation of the new results on the $Mn_xZn_{1-x}F_2$ system.

B. Dynamic scaling

Fisher has shown[13] that for the RFIM, there is a dramatic critical slowing down as $T_c(H)$ is approached, with a characteristic relaxation time τ, diverging with an activated form

$$\tau\sim\exp(C/\mid t-t_c\mid^{\bar{\nu}\theta}) \quad (9)$$

rather than the usual power-law form. Here $\bar{\nu}$ is the correlation length exponent, and θ is the "violation of hyperscaling" exponent, which describes the anomalous growth of the free energy in a correlation volume leading to the modified hyperscaling relation

$$2-\bar{\alpha}=(d-\theta)\bar{\nu}\ . \quad (10)$$

The specific heat is expected to scale, for $T\to T_c$, as

$$C_m\sim\mid t-t_c\mid^{-\bar{\alpha}}f((\ln\omega)/\xi^{\theta})\ , \quad (11)$$

where f is a universal scaling function. At the critical point, C_m must be independent of ξ, thus

$$(C_m)_p\sim\mid\ln\omega\mid^{\bar{\alpha}/\bar{\nu}\theta}\ . \quad (12)$$

The apparent width of the transition t^* due to finite frequency measurements should scale as

$$t^*\sim\mid\ln\omega\mid^{-1/\theta\bar{\nu}}\ . \quad (13)$$

If the random field is small (as is the case in the experiments), the critical behavior near T_c will also be affected by the crossover from the REIM fixed point at $H=0$, $T=T_N$. Equation (11) is then valid if lengths are measured in units of the crossover length $L_0\sim\xi_{\mathrm{cr}}\sim t_{\mathrm{cr}}^{-\nu}\sim h_{\mathrm{RF}}^{-2\nu/\phi}$ and times in units of $\tau_0\sim L_0^z$, where ν and z (the dynamic scaling exponent) correspond to zero-random-field exponents. This guarantees that along the RFIM-REIM crossover boundaries defined by Eq. (1), Eq. (11) becomes equal to the REIM expression

$$C_m \sim |t|^{-\alpha} f'(\omega \xi_{\rm cr}^z) , \quad (14)$$

verifying that both static and dynamic functions match along the crossover lines. Equation (11) then becomes

$$C_m \propto h_{\rm RF}^{-2(\alpha-\bar{\alpha})/\phi} |t-t_c|^{-\bar{\alpha}} \times f[\ln(\omega h_{\rm RF}^{-2\nu z/\phi})(|t-t_c| h_{\rm RF}^{-2/\phi})^{\bar{\nu}\theta}] . \quad (15)$$

The apparent rounding half-width, $|t-t_c|^* \equiv t^*$, caused by measurements at finite frequency scales as

$$t^* \propto h_{\rm RF}^{2/\phi}[\ln(\omega h_{\rm RF}^{-2\nu z/\phi})]^{-1/\bar{\nu}\theta} \quad (16)$$

and the amplitude of the peak in C_m is

$$(C_m)_p \propto h_{\rm RF}^{-2\alpha/\phi}[\ln(\omega h_{\rm RF}^{-2\nu z/\phi})]^{\bar{\alpha}/\bar{\nu}\theta} , \quad (17)$$

where the $h_{\rm RF}^{-2\alpha/\phi}$ factor arises from the field dependence of the static scaling of C_m [Eq. (4)]. Thus we have the result, except for logarithmic corrections in $h_{\rm RF}$ and ω, that the dynamics and static scaling are the same, i.e.,

$$t^* \propto h_{\rm RF}^{2/\phi} \text{ and } (C_m)_p \propto h_{\rm RF}^{-2\alpha/\phi} . \quad (18)$$

The "width" of C_m scales as does the static temperature scaling, and the peak height scales as does the amplitude of the divergence at t_c. The same observation applies to both components of $d(\Delta n)/dT$, i.e., the peak height of each component scales with $h_{\rm RF}$ as $h_{\rm RF}^{y}$, with $y=0.13$ and $y'=1.56$, respectively.

This is in fact a general result. A thermodynamic function F can be written in terms of the scaled temperature, as in Eq. (4),

$$F \propto h_{\rm RF}^{y}(|t-t_c| h_{\rm RF}^{-2/\phi})^{x} f' .$$

Here f' is a dynamic scaling function of the argument of f in Eq. (15), which describes the dynamic rounding of F for $|t-t_c| \le t^*$. F can be transformed to

$$F \propto h_{\rm RF}^{y}[\ln(\omega h_{\rm RF}^{-2\nu z/\phi})]^{x/\bar{\nu}\theta} \times f''[\ln(\omega h_{\rm RF}^{-2\nu z/\phi})(|t-t_c| h_{\rm RF}^{-2/\phi})^{\bar{\nu}\theta}] , \quad (19)$$

where f'' is now a function which describes the complete profile of F: *both* the static scaling and the dynamic rounding for $|t-t_c| \le t^*$. We see that the usual static $|t-t_c| h_{\rm RF}^{-2/\phi}$ term dominates the scaling behavior, with only logarithmic corrections in ω and $h_{\rm RF}$. Likewise, the peak amplitude scales as does the static scaling with $h_{\rm RF}^{y}$, with only logarithmic corrections in ω and $h_{\rm RF}$.

III. EXPERIMENTAL METHODS AND SAMPLE CHARACTERIZATION

The optical birefringence (Δn) technique has been extensively used for studies of optically transparent magnetic materials.[14–16] The proportionality between $d(\Delta n)/dT$ and C_m has been exploited, for example, in studies of the pure Ising,[17] REIM,[18] and RFIM (Ref. 19) problems. The method is particularly well suited to critical phenomena investigations in *mixed* (i.e., random, two component) crystals, where inevitable macroscopic concentration gradients produce undesirable rounding of the phase transition. For the $Fe_xZn_{1-x}F_2$ system, in a further application of the Δn technique, the room-temperature birefringence has been used both to characterize the concentration gradient in a given crystal and to choose the crystal (or portion thereof) with the smallest gradient for subsequent critical phenomena studies, either using birefringence or other methods (e.g., susceptibility or neutron scattering).[20,21]

The gradient characterization method using the ambient temperature Δn technique does require the endpoint components (e.g., FeF_2 and ZnF_2) to have values of Δn which differ sufficiently from each other so that small variations in concentration of the alloy (e.g., $Fe_xZn_{1-x}F_2$) will be manifest as large birefringence variations in the mixed crystal. This condition is well satisfied for $Fe_xZn_{1-x}F_2$ but not for the $Mn_xZn_{1-x}F_2$ system (see the extensive discussion in Ref. 20).

Despite not being able to characterize the gradient at ambient temperature in the $Mn_xZn_{1-x}F_2$ crystals via the Δn technique, one can nevertheless use it to obtain some measure of the axial concentration gradient by examining both the mean transition temperature $\bar{T}_N$ as a function of position along the crystal boule axis and the apparent *rounding* of the transition itself from an analysis of the critical behavior (see extensive discussion in Ref. 21). This one does by measuring $d(\Delta n)/dT$ versus T in the vicinity of T_N, focusing a collimated (≈ 0.2 mm diameter) laser beam *perpendicular* to the growth axis. This allows one to minimize the effects of the predominant concentration gradient (typically $\sim 1\%$ per centimeter) along the crystal growth axis, though not those due to radial gradients. In each $Mn_xZn_{1-x}F_2$ crystal studied we have used this method to optimize the choice of axial position for the detailed measurements of $d(\Delta n)/dT$ versus T which are reported below (see discussion below of Fig. 1).

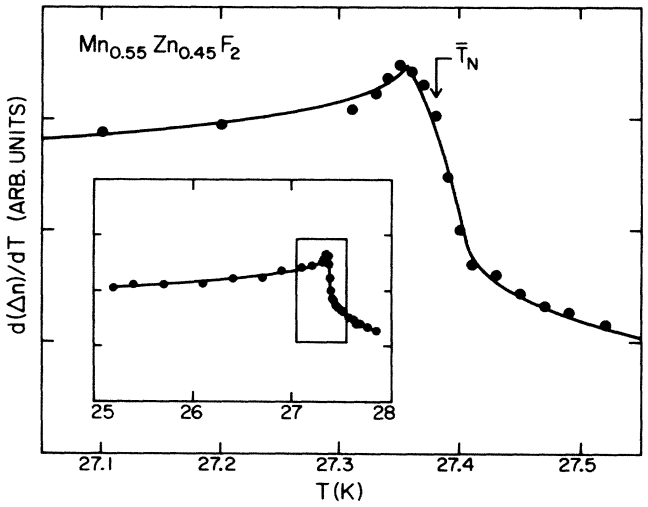

FIG. 1. Inset shows temperature derivative of the optical birefringence $d(\Delta n)/dT$ vs T in $Mn_{0.55}Zn_{0.45}F_2$ at $H=0$. In the main part of the figure $d(\Delta n)dT$ vs T is displayed for the critical region (indicated by the box in the inset). The solid line is the best-fit REIM critical behavior, including the effects of an assumed linear concentration gradient which causes a rounding of $\delta T_N = 0.050 \pm 0.005$ in T_n. Note the peak value of $d(\Delta n)/dT$ does not occur at the average Néel temperature $\bar{T}_N$.

Three $Mn_xZn_{1-x}F_2$ crystals were studied. Their concentrations ($x=0.40$, 0.55 and 0.83) were determined by density measurements within an estimated accuracy in x of ± 0.01. Although earlier measurements[22] of $T_N(x)$ for x very close to one showed the *initial* slope $1/T_N(1)(dT_N/dx)_{x\simeq 1}=1$, the values of T_N obtained from the $d(\Delta n)dT$ measurements are consistent with a linear change of T_N, in the range $0.4\leq x\leq 0.83$, approximately given by $T_N(x)=T_N(1)(x-x_p)/(1-x_p)$, where $x_p=0.24$ is the percolation concentration. This non-Ising-like property of the $Mn_xZn_{1-x}F_2$ system is to be contrasted with that of $Fe_xZn_{1-x}F_2$ for which $1/T_N(1)(dT_N/dx)=1$ over the entire range $0.3\leq x\leq 1$,[23] as would be expected for an Ising system.

The crystals were x-ray oriented and mounted with the c axis colinear with the applied magnetic field H to within $\pm 1°$. The experimental birefringence apparatus has been previously described.[17] The magnetoresistance of the calibrated carbon-glass thermometer was separately measured and taken into account in the field dependent $d(\Delta n)/dT$ studies. the short-term temperature stabilization was better than 1 mK. In order to rule out any possible thermometer drift between runs done on the same sample on consecutive days, we remeasured $d(\Delta n)/dT$ versus T at $H=0$ and compared this result with the corresponding data previously obtained under the same conditions. When keeping the thermometer below $T=100$ K we found the differences to be of the order of 10 mK. The magnetic field was calibrated using NMR.

It has now been well established[2,4,5] that field cooling (FC) of a $d=3$ RFIM system results in the quenching in of a nonequilibrium domain state. Hence all of the $d(\Delta n)/dT$ data were taken by first zero field cooling (ZFC) the crystal to well below T_N, and then raising the field to the desired value. The critical behavior was then explored by either heating the crystal at constant H [to obtain $d(\Delta n)/dT$ versus T], or monotonically increasing H at constant T [to obtain $d(\Delta n)/dH$ versus H] on through the phase transition region.

IV. EXPERIMENTAL RESULTS

The temperature derivative of the optical birefringence $d(\Delta n)/dT$ was studied in three selected crystals of $Mn_xZn_{1-x}F_2$ ($x=0.40$, 0.55, and 0.83). We first discuss the observed behavior of $d(\Delta n)/dT$ at $H=0$ so as to understand the nature of the singularity in the specific heat and the effects of a concentration gradient upon it. Next, we present the field dependence of $d(\Delta n)dT$ versus T and abstract the crossover exponent ϕ for each of the three crystals. Then we consider the scaling behavior of the dynamic rounding of the phase transition in $Mn_{0.55}Zn_{0.45}F_2$. Finally, we derive the complete phase diagram for the special case of $Mn_{0.40}Zn_{0.60}F_2$ as obtained from measurements of $d(\Delta n)/dT$ versus T at constant H and $d(\Delta n)/dH$ versus H at constant T.

A. Behavior of $d(\Delta n)/dT$ versus T at $H=0$

As noted above, scans of $d(\Delta n)/dT$ were made along the growth axis of the three crystals to find the particular region in each one in which the transition appeared sharpest. The optimum result for the $Mn_{0.55}Zn_{0.45}F_2$ crystal is displayed in Fig. 1. The inset shows all of the data for the region around the phase transition, whereas the main part of the figure displays the critical behavior of $d(\Delta n)/dT$ just in the region of reduced temperature $|t|\leq 10^{-2}$. The data looks virtually identical to previously obtained results on $d(\Delta n)/dT$ versus T in the $Fe_xZn_{1-x}F_2$ system.[18] In the latter case the critical behavior was analyzed as belonging to the REIM universality class, for which the exponent α in $C_m=A^{\pm}|t|^{-\alpha}$ has the value $\alpha=-0.09\pm 0.03$ and the amplitudes $A^+(t>0)$ and $A^-(t<0)$ have a ratio $A^+/A^-=1.6\pm 0.3$.

In two recent works King *et al.*[20] and Belanger *et al.*[21] have demonstrated by direct measurement and simulation what are the effects that a *linear* concentration gradient has on the rounding of the phase transition as determined by $d(\Delta n)/dT$ studies. We use their procedures to fit the data shown in Fig. 1. The exponent is fixed at $\alpha=-0.09$ and the amplitude ratio $A^+/A^-=1.7$ is chosen. The assumed linear gradient in T_N, δT_N, and the average transition temperature $\bar{T}_N$ were allowed to vary until a best fit was obtained, which corresponded to $\delta T_N=0.050\pm 0.005$ K and $\bar{T}_N=27.381\pm 0.003$ K. This is shown by the solid line in Fig. 1. It is essential to note that the maximum of $d(\Delta n)/dT$ versus T does *not* occur at $\bar{T}_N$ as has been pointed out to be the case in any instance in which a concentration gradient is present and $A^+/A^-\neq 1$, irrespective of the sign of α[21]. For the other two crystals we estimated the values of $\bar{T}_N=12.55\pm 0.05$ K ($Mn_{0.40}Zn_{0.60}F_2$) and $\bar{T}_N=52.355\pm 0.005$ K ($Mn_{0.83}Zn_{0.17}F_2$). The greater uncertainty in $\bar{T}_N$ in the 40% Mn crystal comes, in part, from the rapid decrease in the amplitude $A^{\pm}$ of the singularity in C_m with increasing dilution, making the experimental signal-to-noise ratio poorer than it is at higher Mn concentrations. The values of $\bar{T}_N$ versus x so obtained are in accord with earlier[3,4] and recent[24] measurements in the $Mn_xZn_{1-x}F_2$ system, but not with the recent results of Ikeda.[25] Pertinent data are collected in Table I.

B. Determination of $T_c(H)$ and ϕ

The field dependence of $d(\Delta n)/dT$ versus T with $H\|c$ axis, was measured in each of the three crystals. Representative data for the $Mn_{0.40}Zn_{0.60}F_2$, $Mn_{0.55}Zn_{0.45}F_2$ and $Mn_{0.83}Zn_{0.17}F_2$ crystals are shown in Figs. 2, 3, and 4, respectively, at a few of the many fields measured. As we found in earlier[19,26] studies of the $Fe_xZn_{1-x}F_2$ system, the shape of $d(\Delta n)/dT$ versus T becomes increasingly symmetric around $T_c(H)$ as the field is raised. This has been interpreted as arising from a symmetric logarithmic divergence in $|t-t_c|$. The apparent increase in rounding of the transition as H increases is a direct consequence of static scaling and extreme critical slowing down effects inherent to the RFIM problem[13] (see discussion below).

Unlike the asymmetric case, the peak of a symmetric singularity *does* occur at $\bar{T}_c(H)$ in the presence of a con-

TABLE I. Parameters obtained for $Mn_xZn_{1-x}F_2$ system. The quantities $\bar{T}_N$, b, C, and ϕ are defined in the text and correspond to least-squares fits of $T_c(H)$ to Eq. (3) (unless otherwise specified). In the last column we quote the resulting root-mean-square deviation (rms) of the data with respect to the fitted curve.

x	$\bar{T}_N$ (K)	b (10^{-10} K/Oe^2)[a]	C (K/kOe$^{2/\phi}$)	ϕ	rms (mK)
0.40	12.55(5)[b]	3.9	$1.6(2)\times10^{-1}$	1.45(14)	50
	12.56(14)[c]		$1.6(7)\times10^{-1}$	1.46(21)	50
0.55	27.381(3)[b]	2.9	$3.2(1)\times10^{-2}$	1.44(3)	3
	27.384(7)[c]		$3.3(3)\times10^{-2}$	1.46(5)	3
0.83	52.355(5)[b]	1.9	$3.7(4)\times10^{-3}$	1.36(8)	3
	52.357(10)[c]		$3.9(1.3)\times10^{-3}$	1.38(10)	3

[a]Taken to be $b(x)=x^{-1}b(1)$, where $b(1)=1.57\times10^{-10}$ K/Oe^2. If instead $b(x)$ is calculated from $b(x)=b(1)T_N(1)/T_N(x)$, the results for ϕ increase by $\lesssim 1\%$ in all cases.
[b]Fixed. The uncertainty in ϕ includes the statistical error of the fitting procedure as well as the variations of ϕ produced by changing T_N by $\pm\delta T_N$.
[c]Taken as free parameters.

centration gradient. Thus no elaborate fitting procedure is required to determine $\bar{T}_c(H)$ versus H away from $H=0$. For the three crystals, the raw $\bar{T}_c(H)$ versus H data were "mean-field" corrected through the bH^2 term given in Eq. (3), with $b(x)=x^{-1}b(1)$ (see Table I). The quantity $\bar{T}_N-\bar{T}_c(H)-bH^2$ versus H is shown in a log-log plot in Fig. 5. The values of ϕ, C, and $\bar{T}_N$ determined from a least-squares fit to Eq. (3) are given in Table I.

Some remarks are in order concerning the different uncertainties that enter into the determination of ϕ in each case. For $x=0.83$, the bH^2 term makes a proportionately larger contribution to the small shift in $\bar{T}_c(H)$, relative to the $CH^{2/\phi}$ term, than it does for $x=0.55$ and 0.40. Hence the accuracy to which ϕ can be determined at $x=0.83$ depends on how well one believes the mean-field correction can be made and how accurately $\bar{T}_N$ is determined. If either the form $b(x)=x^{-1}b(1)$ or $b(x)=[T_n(1)/T_N(x)]b(1)$ is used and $\bar{T}_N$ is fixed (i.e., including the $H=0$ point) then $\phi=1.37\pm0.08$ is obtained. If $\bar{T}_N$ is taken as a free parameter, (i.e., excluding the $H=0$ point), the best fit gives $\bar{T}_N=52.357\pm0.010$ and $\phi=1.38\pm0.10$. The value of T_N obtained this way is in excellent agreement with the $H=0$ fitting of the data, and is a further verification of the validity of the procedure.

At the opposite extreme is $Mn_{0.40}Zn_{0.60}F_2$ where the shift in $T_c(H)$ is large and the bH^2 is proportionately less important. Fixing T_N to $\bar{T}_N\pm\delta T_N$ and restricting the range of fields to $0\le H\le 6$ kOe yields a value of $\phi=1.45\pm0.14$. Leaving $\bar{T}_N$ as a free parameter results in almost identical values of ϕ and $\bar{T}_N$ but with still larger uncertainties; $\phi=1.46\pm0.21$ and $\bar{T}_N=12.56\pm0.14$. Why is one not able to capitalize on the large random-field shift to obtain a more precise value of ϕ? At the low Mn

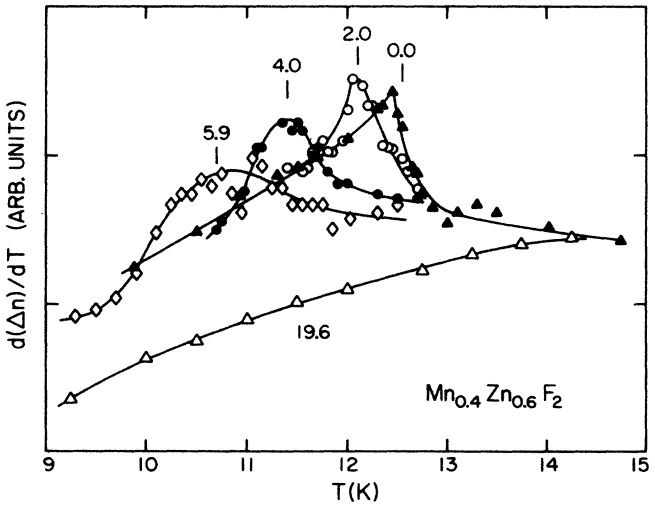

FIG. 2. $d(\Delta n)/dT$ vs T in $Mn_{0.40}Zn_{0.60}F_2$ at $H=0$, 2.0, 4.0, 5.9, and 19.6 kOe. The average transition temperatures are indicated by vertical lines. The curves are guides to the eye.

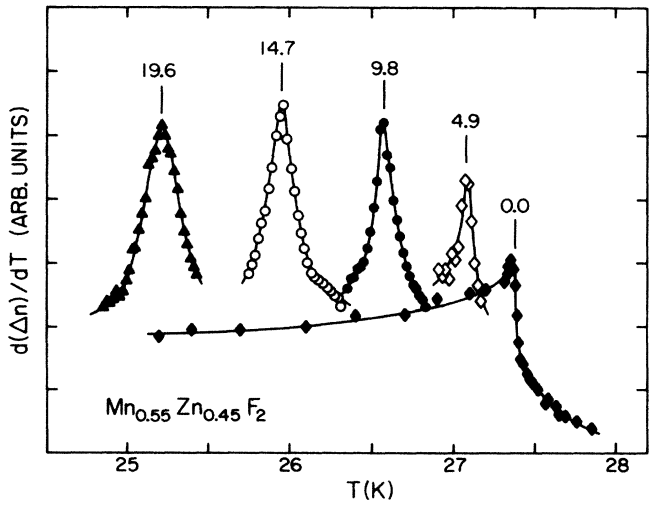

FIG. 3. $d(\Delta n)/dT$ vs T in $Mn_{0.55}Zn_{0.45}F_2$ at $H=0$, 4.9, 9.8, 14.7, and 19.6 kOe. The average transition temperatures are indicated by vertical lines. The curves are guides to the eye.

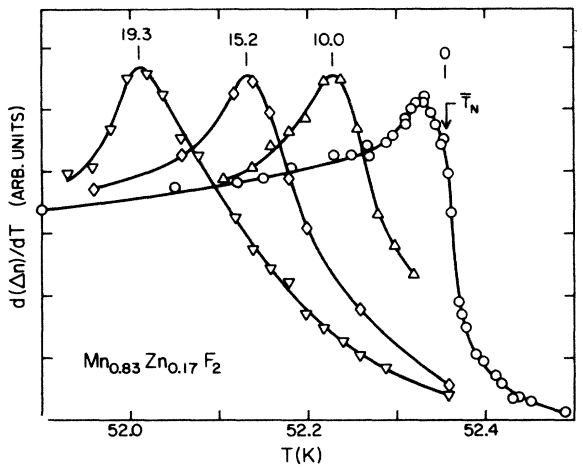

FIG. 4. $d(\Delta n)/dT$ vs T in $Mn_{0.83}Zn_{0.17}F_2$ at $H=0$, 10.0, 15.2, and 19.3 kOe. The average transition temperatures are indicated by vertical lines. The curves are guides to the eye.

concentration two factors contribute to the increased error in the determination of ϕ: one is the rapid decrease in the amplitudes $A^{\pm}$ with decreasing x (much faster than x^2, as one might näively expect), and the other is the increase of the dynamic rounding of the phase transition with decreasing x, at a constant H. Both factors cause increased uncertainty in the determination of $T_c(H)$ because of poorer signal-to-noise ratios. Added to all of the above is the limited field range ($0 \leq H \leq 6$ kOe) in which the shift can be described by Eq. (3). We will return to this latter point in the discussion of the complete H-T phase diagram for $Mn_{0.40}Zn_{0.60}F_2$.

For $Mn_{0.55}Zn_{0.45}F_2$ fixing the Neel temperature to $\bar{T}_N = 27.381 \pm 0.003$ we obtained $\phi = 1.44 \pm 0.03$. Even allowing $\bar{T}_N$ to be an adjustable parameter (i.e., excluding the $H=0$ point) gives $\phi = 1.46 \pm 0.05$ and $\bar{T}_N = 27.384 \pm 0.007$ K, both very close to the values obtained with $\bar{T}_N$ fixed. In order to obtain an upper limit to the uncertainty in ϕ we have allowed b to change by 50% and $\bar{T}_N$ to vary by ± 5 mK leading to a value of $\phi = 1.44 \pm 0.07$. Considering the pros and cons of the other two concentrations, the $Mn_{0.55}Zn_{0.45}F_2$ crystal is clearly the best of the three for the accurate determination of ϕ.

From a comparison of the best value of ϕ (see Table I) obtained for each crystal, it appears that no variation of ϕ with x occurs in the range $0.4 \leq x \leq 0.83$, within the combined experimental errors. If we assumed that no variation in ϕ with x is to be expected then we make a weighted average of the three measurements of ϕ; in which case $\bar{\phi} = 1.43$ with a variance of ± 0.03.

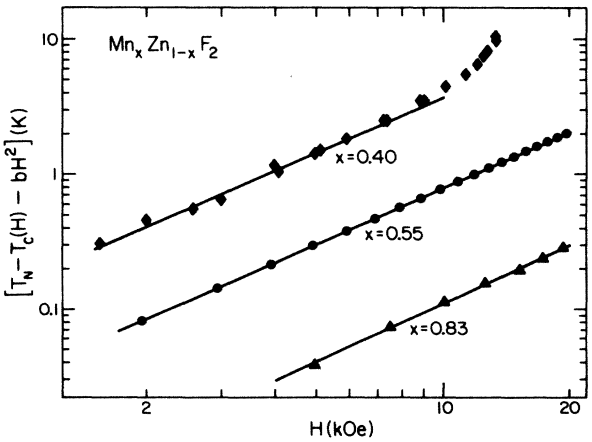

FIG. 5. Log-log plot of the mean-field-corrected shift in $T_c(H)$ from T_N vs H in the $Mn_xZn_{1-x}F_2$ systems. The solid lines are the best power-law fits and yield the values of ϕ given in Table I.

C. Rounding of the transition in an applied field: inhomogeneous broadening, static and dynamic scaling effects

Previous $d\Delta n/dT$ experiments[19] have shown that the shape of the transition in the RFIM regime can be well described as a logarithmic divergence [i.e., $d(\Delta n)/dT \propto \log|T - T_c(H)|$]. For low fields a rounding of this logarithmic behavior can be expected at $|T - T_c(H)| < \delta T_N$ where δT_N is the rounding of the transition at $H=0$ caused by a concentration variation δx, The dependence of the parameter C of Eq. (3) on x will induce an additional rounding of $T_c(H)$. For $Mn_{0.55}Zn_{0.45}F_2$ we estimate this contribution to be

$$\delta T_c(H) \approx 0.1[T_N - T_c(H) - bH^2]\delta T_N \ .$$

The total rounding of $T_c(H)$ due to inhomogeneities would then be

$$\delta T_c \approx \delta T_N\{1 + 0.1[T_N - T_c(H) - bH^2]\}$$

in this crystal.

Besides rounding from inhomogeneities, dynamical rounding[27,13] has been shown[28] to play an important role in determining the response of the system in the critical region. Although the present experiments are nominally "dc" or steady-state measurements, they were actually carried out on a finite time scale of $\tau \approx 100$ sec per measurement. The critical slowing down in RFIM systems is so extreme that even on the time scale, $\omega \approx 1/\tau \approx 10^{-2}$ sec^{-1}, dramatic dynamic effects are expected.[29,30] For $|t - t_c| < t^*$ given by Eq. (18), the logarithmic critical divergence is expected to be limited, and the peak in $d(\Delta n)/dT$ to approach a finite value given by Eq. (18). We assume, in the case of a logarithmic divergence, that the singular part of the peak amplitude is given in Eq. (17) with $\bar{\alpha} \to 0$, which leads to only log-log corrections in ω and h_{RF} to be applied to Eq. (18). In practice, it is not possible to distinguish experimentally between a very small value of $\bar{\alpha}$ and $\log|t - t_c|$, nor would it be possible to distinguish between the two forms of Eq. (17).

To compare the data with these predictions, we show in Fig. 6 a typical semilog plot of the amplitude for $Mn_{0.55}Zn_{0.45}F_2$ at 19.6 kOe together with an estimation of t^*, defined as the reduced temperature at which the asymptotic logarithmic behavior intercepts a horizontal line drawn through the peak. Assuming $t^* \propto H^{2/\phi}$ [Eq. (18)], the dynamic rounding of $T_c(H)$ would be $t^* T_N$, with $t^*(H = 19.6$ kOe, $\tau = 100$ sec$) = 2.2 \times 10^{-3}$ as es-

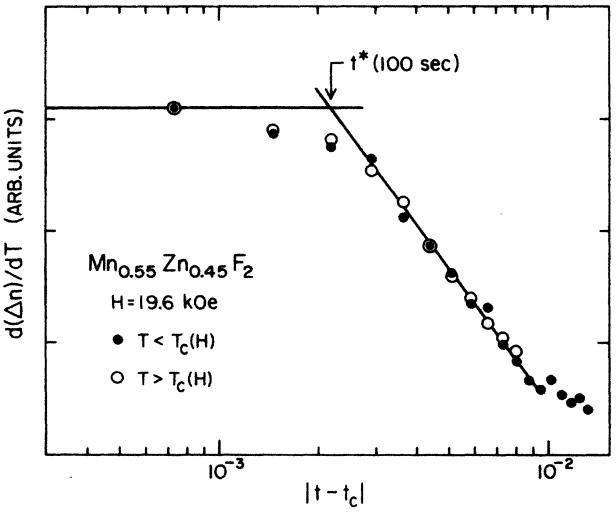

FIG. 6. Semilog plot of $d(\Delta n)/dT$ vs reduced temperature $t-t_c$. The construction by which the effective dynamic rounding temperature t^* is determined is explained in the text and follows the procedures used to analyze the ac susceptibility (Ref. 28) and Faraday rotation (Ref. 29) in the $Fe_xZn_{1-x}F_2$ system.

timated from Fig. 6.

The field-dependent peak-amplitude scaling of Eq. (18) cannot be simply compared with the data because the measurement of the amplitude requires a reference base line. We construct the latter by noticing that the crossover boundary t_{cr}, Eq. 1, and t^* both scale with h_{RF} as $h_{RF}^{2/\phi}$. Thus the values of the scaling function of Eq. (4) at these points are field independent, and the corresponding values of C_m scale with h_{RF} with only the explicit field dependence of C_m. We note that the RFIM value of C_m crosses over to the REIM value at t_{cr}^- (the low-temperature crossover) and that the REIM value of C_m is only weakly temperature dependent between t_{cr}^- and $T_c(H)$. It is reasonable to conclude from this that the height of the RFIM peak above the $H=0$ data should be a good measure of the field-dependent amplitude of $d(\Delta n)/dT$.

The effect of concentration gradient on the peak height and width is expected to be largest at low fields, where $t^*T_N < \delta T_N$, becoming negligible at larger fields, where $t^*T_N \gg \delta T_N$. To take this variation into account, we use the following model to treat the static and dynamic effects together: in the absence of a gradient, we approximate the peak profile by

$$d(\Delta n)/dT \propto H^{-2\alpha/\phi} \log \frac{[(T-T_c)^2+(t^*T_N)^2]^{1/2}}{kH^{2/\phi}} . \quad (20)$$

Here $k=0.007$ K/(kOe)$^{2/\phi}$ is chosen to fit the data with $d(\Delta n)/dT \to 0$ at t_{cr}^-.

The effects of the gradient on this expression are then approximated by integrating $T_c(H)$ over the range $(\bar{T}_c-\delta T_c) \le T_c(H) \le (\bar{T}_c+\delta T_c)$. The peak amplitude at $T=\bar{T}_c$ is found to be

$$d(\Delta n)/dT \propto H^{-2\alpha/\phi} \left[\log \frac{[\delta T_c^2+(t^*T_N)^2]^{1/2}}{kH^{2/\phi}} - 1 + \frac{t^*T_N}{\delta T_c} \tan^{-1}\left[\frac{\delta T_c}{t^*T_N}\right] \right] . \quad (21)$$

For low fields, where $t^*T_N < \delta T_c$, the limits of integration are taken to be $\bar{T}_c \pm t^*T_N$ since $d(\Delta n)/dT$ [Eq. (20)] is assumed to be zero outside this range.

In Fig. 7 we have plotted the amplitude of the peaks taken as the maximum in $d(\Delta n)/dT$ measured with respect to the $H=0$ curve at the same temperature. These results can be compared with the evaluation of Eq. (21) (lower curve in Fig. 7), where we have used the previously estimated magnitude for δT_N and t^*. Only the proportionality constant in Eq. (21) was taken as an adjustable value. In order to have an estimate of the effect of the inhomogeneities on the peak amplitude we have set $\delta T_N = 0$ and left the remaining parameters fixed: this is shown by the upper curve in Fig. 7. This simple analysis shows the importance of considering the effects of concentration variations and the critical slowing down when analyzing the critical behavior of the RFIM systems.

As an inset to Fig. 7 we show the prediction of the line shapes for the transitions at different fields found by integrating Eq. (20) with the same parameters used to calculate the peak amplitude. Since for the region

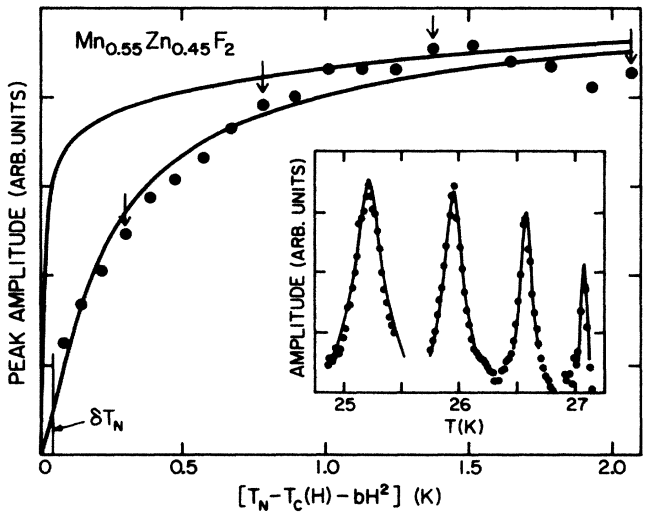

FIG. 7. Peak amplitude of $d(\Delta n)/dT$ vs the mean-field corrected shift in $T_c(H)$ at several values of $H \neq 0$ in $Mn_{0.55}Zn_{0.45}F_2$. The upper curve is the expected weak random-field $H^{0.13}$ scaling in the absence of gradient rounding. The lower curve is the result of a calculation that takes into consideration the measured gradient induced rounding of $\bar{T}_N$. δT_N is the rounding observed at $H=0$ as was determined in the best fit to the critical behavior shown in Fig. 1. The inset shows the complete $d(\Delta n)/dT$ data at $H=4.9$, 9.8, 14.7, and 19.6 kOe (indicated by the arrows in main figure) in the RFIM region. The solid lines are the calculated behavior of $d(\Delta n)/dT$ vs T at each value of H and include static and dynamic scaling effects as well as those arising from the concentration gradient induced rounding.

$|T-T_c(H)| > t^*T_N$ the amplitude is entirely determined by static scaling it is clear that the increase in the apparent width of the transition region with magnetic field is a direct consequence of static and not dynamic scaling. Note that the apparent width (half width at half height) is not to be confused with t^*T_N, which is a much smaller quantity.

D. Complete H-T phase diagram for $Mn_{0.40}Zn_{0.60}F_2$

In the $Mn_{0.40}Zn_{0.60}F_2$ crystal we were able to examine the nature of the phase boundary between $2 < T \leq 13$ K. This was accomplished by measuring $d(\Delta n)/dT$ versus T at constant H (see Fig. 2) and $d(\Delta n)/dH$ versus H at constant T (see Fig. 8). The combined results of the two kinds of measurements of $T_c(H)$ versus H are shown in Fig. 9. By extrapolation to $T=0$ of a smooth curve through the data, one can surmise that $(dH_c/dT)_{T=0}=0$, and that the critical field at $T=0$ is $H_c=13.8$ kOe. Furthermore, from the monotonically changing character of the data of Figs. 2 and 8 the continuous curvature of $T_c(H)$ versus T, we deduce that no other critical points appear along the phase boundary. Hence the transition, which is second-order at the smallest fields, appears to remain second-order along the entire boundary.

Since the $Mn_xZn_{1-x}F_2$ system exhibits a bicritical point at a value of x at least as small as 0.5,[31] we searched for a spin-flop–paramagnetic transition by measurement of $d(\Delta n)/dT$ versus T in the range $1.9 \leq T \leq 20$ K at various fields between $14 \leq H \leq 20$ kOe. The result of part of the 19.6 kOe scan is shown in Fig. 2. No evidence for any other phase–boundary line was found.

The inset to Fig. 9 shows the same phase boundary but plotted as $H^{2/\phi}$ versus T. The straight line through the high-temperature points is the best-fit-of the $H < 6$ kOe data shown in the log-log plot of Fig. 5. Clearly one rapidly departs from the predictions of Eq. (3) as H increases above 6 kOe. For this weakly Ising system, the extent of the field range of simple RFIM behavior is noticeably smaller than that of the more Ising-like $Fe_xZn_{1-x}F_2$ system where even for $x=0.46$ one observes $H^{2/\phi}$ behavior, to 20 kOe at least.[26]

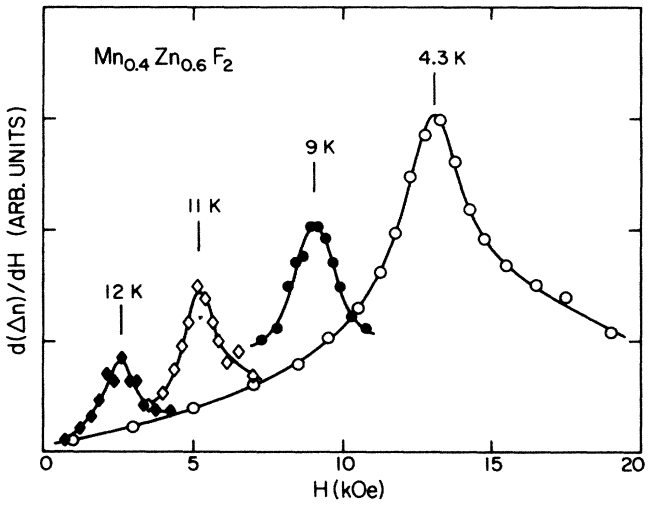

FIG. 8. Field derivative of the optical birefringence $d(\Delta n)/dH$ vs H in $Mn_{0.4}Zn_{0.6}F_2$ at temperatures $T=4.3$, 9, 11, and 12 K. The lines are guides to the eye.

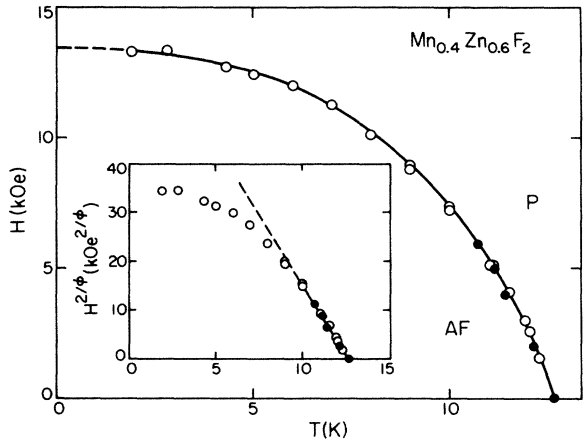

FIG. 9. Complete phase diagram for $Mn_{0.4}Zn_{0.6}F_2$. Solid dots were obtained from $d(\Delta n)/dT$ vs T and the open circles from $d(\Delta n)/dH$ vs H measurements. The solid line is a best fit to the data for $H < 6$ kOe and a guide to the eye at larger fields. The dashed portion is an extrapolation of it to $T=0$ K. The inset is the same data in an $H^{2/\phi}$ vs T plot, showing where the departure from the weak random-field behavior first occurs.

V. COMPARISON OF NEW RESULTS WITH EARLIER STUDIES OF $d=3$ RFIM SYSTEMS

Until very recently, the experimental situation on ϕ has appeared to be ambiguous. Seemingly differing results had been obtained for the three primary $d=3$ RFIM systems studied: $Fe_xZn_{1-x}F_2$,[2] $Mn_xZn_{1-x}F_2$,[3] and $Fe_xMg_{1-x}Cl_2$.[5] FeF_2 has a single predominant intersublattice exchange and a large, single-ion, easy-axis anisotropy, making it an ideal $d=3$ pure Ising system. Measurements of the critical exponents of FeF_2 are in good agreement with pure Ising values throughout the entire critical region.[32] Values of ϕ from measurements of the of the optical birefringence [$\phi=1.40\pm0.05$ (Ref. 18); 1.42 ± 0.03 (Ref. 26)], capacitance[33] ($\phi=1.40\pm0.05$), and Faraday rotation[29]($\phi=1.44\pm0.04$) are all in excellent agreement, within experimental error. Recent neutron scattering measurements,[30] on a virtually gradient-free $Fe_{0.46}Zn_{0.54}F_2$ crystal, showed that $\gamma=1.31\pm0.03$, from which it was determined that $\phi/\gamma=1.08\pm0.05$ consistent with Aharony's estimate[12] of $1.05 \leq \phi/\gamma \leq 1.10$.

In $FeCl_2$, a predominant ferromagnetic exchange within the layers, and a weaker antiferromagnetic interaction between layers result in a system with a metamagnetic transition below a tricritical point. The diluted material $Fe_xMg_{1-x}Cl_2$ also exhibits a reduction in T_N which is quasi-two-dimensional, initially decreasing linearly from $x=1$ toward the percolation limit for a $d=2$ square lattice at $x_p \sim 0.5$. Furthermore, the competition between intralayer and interlayer interaction results in a spin-glass phase appearing well above x_p. All the above not withstanding, $FeCl_2$ *does* exhibit three-

dimensional Ising behavior. Therefore, for the diluted material we expect it to exhibit REIM critical behavior.

Specific-heat measurements[5] of the phase diagram of $Fe_{0.682}Mg_{0.318}Cl_2$ showed a peak which was interpreted to shift with an apparent exponent $\phi=1.26\pm0.10$, a value presumably in agreement with $\gamma_p=1.24$. However, there was apparently no attempt to do a critical behavior analysis of the data, nor to make any direct measurement of the effects of a concentration gradient on the determination of $\bar{T}_N$.

More recently, however, very careful Faraday rotation measurements by Leitão and Kleemann[6] on $Fe_{0.7}Mg_{0.3}Cl_2$ have given an exponent $\phi=1.41\pm0.05$ in agreement with the $Fe_xZn_{1-x}F_2$ results. Because of the high sensitivity of the Faraday rotation in this sample, the authors were able minimize the volume of the crystal to ≈ 0.1 mm^3 and therefore reduce the rounding of the transition by gradients of concentration to $\delta T_N/T_N < 1.5\times10^{-3}$. This result for $\delta T_N/T_N$ is of the order of the best result obtained with the birefringence method by orienting a narrow laser beam perpendicular to the concentration gradient, so as to minimize the variation in concentration over the beam. Also, the Faraday rotation experiments were made on a typical time scale of $\tau\approx100$ sec, assuring thermal equilibrium. Finally, only ZFC data were used in determining ϕ. These authors surmized that the results of the earlier specific-heat studies[5] were incorrect since the measurements were made under nonthermal equilibrium conditions, involving averaging ZFC and FC values of the transition temperatures. In addition, no attempt had been made to characterize the necessarily larger concentration gradients that would be present in the size sample required in the heat-capacity measurements. Considering the differences in the manner in which the two studies were made, we believe the Faraday rotation measurements to be more accurate in all respects.

In MnF_2 the exchange interaction is virtually identical to that in FeF_2, but the anisotropy is dipolar and much weaker than the large single-ion anisotropy in FeF_2. Nevertheless, the asymptotic critical behavior of both materials should belong to the same Ising universality class. This was implicit in early birefringence measurements of $Fe_xZn_{1-x}F_2$ and $Mn_xZn_{1-x}F_2$ which gave values of ϕ consistent with $\phi=1.4\pm0.1$ for both systems.[3,4] However, later careful measurements[3] on $Mn_{0.75}Zn_{0.25}F_2$ using the thermal expansion technique gave $\phi=1.25\pm0.07$, consistent with the original idea that $\phi=\gamma_p$. Adding to the dilemma was the fact that neutron scattering measurements[4] on the same crystal determined that the exponents ν and γ were those appropriate to the REIM, not the pure Ising model. So confusing was the experimental situation as to the apparently differing crossover behavior in different systems that some were led to speculate[12] as to whether distinctions existed between "strong" and "weak" Ising systems, which manifest themselves in RFIM crossover behavior, but not in the REIM behavior in the same systems.

It is clear from the present work that the main contribution to the finding of a smaller than expected value of ϕ in the earlier $Mn_{0.75}Zn_{0.25}F_2$ studies was the concentration gradient effect which led the authors to misjudge $\bar{T}_N$ at $H=0$. We can see this effect very readily in our own data at a comparable concentration. For example, in the analysis of $Mn_{0.83}Zn_{0.17}F_2$, we found that if the temperature corresponding to the peak of $d(\Delta n)/dT$ versus T at $H=0$ had been mistakenly chosen as $\bar{T}_n$, the resulting value for ϕ would have been $\phi=1.17\pm0.09$, instead of the value given in Table I. A detailed analysis of gradient effects on critical phenomena are given in the papers by King *et al.*[20] and Belanger *et al.*[21]

On theoretical grounds, however, one might expect the crossover exponent to approach the pure Ising-to-RFIM value of $\phi=\gamma(\text{pure})=1.24$ at very small dilution and very large values of the applied field. For some intermediate range of concentration and applied field, an "effective" exponent might be observed, with a value between those of the pure and REIM-to-RFIM crossovers. Whether or not the slightly smaller (though unchanged within the experimental errors) values of ϕ in the 83% sample is evidence for such a crossover in ϕ cannot be ascertained without further study at higher concentrations and higher fields. The $Fe_xZn_{1-x}F_2$ system would be ideal for this investigation because spin-flop occurs at a much higher field than in the $Mn_xZn_{1-x}F_2$ system.

VI. SUMMARY

When the results obtained for the crossover exponent ϕ in the $Fe_xZn_{1-x}F_2$ system and those recently obtained by Leitão and Kleemann[6] on $Fe_{0.7}Mg_{0.3}Cl_2$ are compared with those reported above for the $Mn_xZn_{1-x}F_2$ system we may conclude that the observed crossover in *all* diluted antiferromagnets is from REIM to RFIM and *not* pure Ising to RFIM behavior. Furthermore, within rather small and well-defined experimental errors, we deduce the following.

(1) ϕ is identical for all three systems ($Fe_xZn_{1-x}F_2$, $\phi=1.42\pm0.03$; $Fe_xMg_{1-x}Cl_2$, $\phi=1.41\pm0.05$; $Mn_xZn_{1-x}F_2$, $\phi=1.43\pm0.03$), within experimental error.

(2) ϕ shows no concentration dependence in the range in which it has been measured in the two systems studied ($Fe_xZn_{1-x}F_2$, $Mn_xZn_{1-x}F_2$).

(3) The Aharony inequality $\phi>\gamma$ (REIM) is well satisfied in these two cases.

It follows that, in the weak random-field limit $[T_N-T_c(H)]\ll T_N$, the static and dynamical critical behavior should be identical for the three systems and should be governed by the same crossover scaling.

ACKNOWLEDGMENTS

We are indebted to N. Nighman for the growth of the $Mn_xZn_{1-x}F_2$ crystals and to D. Huse and Y. Shapira for private communications. One of us (C.A.R.) was supported by the Consejo Nacional de Investigaciones Científicas y Technológicas de la República Argentina. This research was supported by the National Science Foundation Grant No. DMR85-16786.

*Permanent address: Centro Atómico Bariloche, 8400, Bariloche, Río Negro, Argentina.
[1]S. Fishman and A. Aharony, J. Phys. C **12**, L729 (1979).
[2]A. R. King and D. P. Belanger, J. Magn. Magn. Mater. **54-57**, 19 (1986).
[3]Y. Shapira, N. F. Oliveira, Jr., and S. Foner, Phys. Rev. B **30**, 6639 (1984); Y. Shapira and N. F. Oliveira, Jr. *ibid.* **27**, 4336 (1983).
[4]P. W. Mitchell, R. A. Cowley, H. Yoshizawa, P. Böni, Y. J. Uemura, and R. J. Birgeneau, Phys. Rev. B **34**, 4719 (1986).
[5]P. Z. Wong, Phys. Rev. B **34**, 1864 (1986); P. Z. Wong *et al.*, J. Appl. Phys. **53**, 795 (1982).
[6]U. A. Leitão and W. Kleemann, Phys. Rev. B **35**, 8696 (1987).
[7]J. L. Cardy, Phys. Rev. B **29**, 505 (1984).
[8]W. Kleemann, A. R. King, and V. Jaccarino, Phys. Rev. B **34**, 479 (1986).
[9]D. A. Huse (private communication).
[10]Paul H. Barrett, Phys. Rev. B **34**, 3513 (1986).
[11]D. P. Belanger, A. R. King, and V. Jaccarino, Phys. Rev. B **34**, 452 (1986).
[12]A. Aharony, Europhys. Lett. **1**, 617 (1986).
[13]Daniel S. Fisher, Phys. Rev. Lett. **56**, 416 (1986).
[14]J. F. Dillon, Jr., J. Appl. Phys. **20**, 1291 (1958).
[15]A. S. Borovik-Romanov, N. M. Kreines, A. A. Pankov, and M.A. Talalaev, Zh. Eksp. Teor. Fiz. **64**, 1762 (1973) [Sov. Phys.—JETP **37**, 890 (1973)].
[16]I. R. Jahn, Phys. Status Solidi B **57**, 681 (1973).
[17]D. P. Belanger, A. R. King, and V. Jaccarino, Phys. Rev. B **29**, 2636 (1984).
[18]R. J. Birgeneau, R. A. Cowley, G. Shirane, H. Yoshizawa, D. P. Belanger, A. R. King, and V. Jaccarino, Phys. Rev. B **27**, 6747 (1983).
[19]D. P. Belanger, A. R. King, V. Jaccarino, and J. L. Cardy, Phys. Rev. B **28**, 2522 (1983).
[20]A. R. King, I. B. Ferreira, V. Jaccarino, and D. P. Belanger, Phys. Rev. B **37**, 219 (1988).
[21]D. P. Belanger, A. R. King, I. B. Ferreira, and V. Jaccarino, Phys. Rev. B **37**, 226 (1988).
[22]H. Salamati-Mashhad, G. S. Dixon, and J. J. Martin, J. Appl. Phys. **53**, 1929 (1982).
[23]G. K. Wertheim and D. N. E. Buchanan, Phys. Rev. **161**, 478 (1967).
[24]Y. Shapira (private communication).
[25]H. Ikeda, J. Phys. C **19**, L811 (1986).
[26]I. B. Ferreira, Ph.D. thesis, University of California, Santa Barbara, 1987.
[27]J. Villain, Phys. Rev. B **52**, 1543 (1984).
[28]A. R. King, J. A. Mydosh, and V. Jaccarino, Phys. Rev. Lett. **56**, 2525 (1986).
[29]W. Kleemann, A. R. King, and V. Jaccarino, Phys. Rev. B **34**, 479 (1986).
[30]D. P. Belanger, V. Jaccarino, A. R. King, and R. M. Nicklow, Phys. Rev. Lett. **59**, 930 (1987).
[31]Y. Shapira (private communication).
[32]D. P. Belanger and H. Yoshizawa, Phys. Rev. B **35**, 4823 (1987).
[33]A. R. King, V. Jaccarino, D. P. Belanger, and S. M. Rezende, Phys. Rev. B **32**, 503 (1986).
[34]D. P. Belanger, A. R. King, and V. Jaccarino, Phys. Rev. Lett. **48**, 1050 (1982).